

Dynamic Parameter Optimization of High-Speed Pantograph Based on Swarm Intelligence and Machine Learning

Rui Zhou[✉]

*State Key Laboratory of Nonlinear Mechanics
Institute of Mechanics, Chinese Academy of Sciences
Beijing 100190, P. R. China*

*School of Engineering Sciences, University of Chinese Academy of Sciences
Beijing, Beijing 100049, P. R. China
zhou Rui@imech.ac.cn*

Xianghong Xu^{✉*}

*State Key Laboratory of Nonlinear Mechanics
Institute of Mechanics, Chinese Academy of Sciences
Beijing 100190, P. R. China
xxh@lnm.imech.ac.cn*

Received 3 May 2023

Revised 6 July 2023

Accepted 11 July 2023

Published 22 September 2023

Good pantograph–catenary interaction quality is a fundamental premise for ensuring stable and reliable current collection of high-speed trains, and the optimization of dynamic parameters of high-speed pantographs provides an effective approach to improve the current collection quality of the pantograph–catenary system. In this paper, with the objective of minimizing the standard deviation of the pantograph–catenary contact force, the multi-parameter joint optimization for pantograph at different filtering frequencies and running speeds was carried out by using swarm intelligence optimization algorithm and artificial neural network method. First, the selection operator in genetic algorithm (GA) was introduced into crow search algorithm (CSA), and the selective CSA was proposed, which can effectively improve the solution accuracy and convergence rate of multi-parameter optimization. Second, a radial basis function (RBF) neural network was used to construct a surrogate model of the standard deviation of contact force with respect to the running speed and pantograph dynamic parameters, and a method for optimizing the upper limit of mapping interval of the decision variables by the selective crow search algorithm (SCSA) was proposed, which effectively improves the generalization ability of the surrogate model. Finally, by combining the surrogate model and SCSA, optimization iterations for a total of 630 combined conditions such as cut-off frequency, running speed and pantograph dynamic parameters were conducted, and an optimization method for high-speed pantograph dynamic parameters with universal applicability was proposed.

Keywords: Contact force of pantograph–catenary system; selective crow search algorithm; surrogate model; multi-parameter optimization.

*Corresponding author.

1. Introduction

With the increase in the running speed of the train, the issue of the pantograph–catenary dynamic characteristics becomes increasingly noticeable [Bruni *et al.*, 2018]. A good pantograph–catenary contact is essential for ensuring current collection quality for the high-speed train. When the train is running, the strip is in dynamic contact with the catenary, and the vertical contact force generated by the pantograph acting on the catenary is a direct reflection of the pantograph–catenary coupling. The mean value and standard deviation of contact force are used as the main evaluation indexes of the current collection quality [European Parliament, 2012a, 2018, 2020] in line test and numerical analysis. Reasonable contact force is an important quality of the design of pantograph–catenary system. The smaller the standard deviation of contact force is, the smaller the fluctuation of the contact force is, and the better the contact performance of pantograph–catenary system is. Therefore, a good pantograph–catenary relationship requires the standard deviation of contact force to be as small as possible on the premise of satisfying the mean value of contact force, and the standard deviation of contact force is usually used as the objective function in the parameter optimization of pantograph–catenary system.

In recent years, scholars have carried out a lot of work on single-parameter optimization based on the control variable method and multi-parameter optimization based on optimization algorithms for pantograph dynamic parameters. In terms of optimization of a single pantograph parameter, the standard deviation of contact force could be reduced by reducing the equivalent mass of panhead vertical vibration m_3 , increasing the equivalent stiffness of panhead vertical vibration k_3 or the equivalent damping of frame rotation c_1 in the case of CX pantograph, and 300 km/h, and the optimization effect would decrease [Pombo and Ambrósio, 2012]. The standard deviation of contact force could be reduced by reducing k_3 , increasing the equivalent damping of upper frame vertical vibration c_2 or c_1 , and reducing the equivalent stiffness of upper frame vertical vibration k_2 in the case of DSA250 pantograph, and 250 km/h and the optimization effect would decrease [Zhou and Zhang, 2010]. The standard deviation of contact force could also be reduced by reducing m_3 or the equivalent mass of frame rotation m_1 , reducing k_3 or k_2 , increasing c_2 , c_1 , or the equivalent damping of panhead vertical vibration c_3 in the case of DSA380 pantograph, and 350 km/h and m_3 and c_1 have the best optimization effect [Wu *et al.*, 2021].

Existing studies on the optimization of pantograph–catenary dynamic parameters have shown that the effect of multi-parameter joint optimization is significantly higher than that of single-parameter optimization [Wu *et al.*, 2021, 2022]. The work on the optimization of multiple pantograph parameters focuses on two aspects as follows.

First, optimization algorithms are used to determine the samples in each generation and iterate gradually until the objective function reaches the optimal value, which corresponds to the optimal solution of parameters and the standard deviation

of contact force of each samples in each generation during iteration is obtained by pantograph–catenary dynamic calculation. A joint optimization of m_3 , k_3 and c_3 by using genetic algorithm (GA) could reduce the standard deviation of contact force by 11.0%, and the optimization direction was to reduce m_3 and increase k_3 and c_3 [Ambrósio *et al.*, 2013]. Combined GA and basic descent method, the joint optimization of eight pantograph parameters except m_3 at 250, 300 and 350 km/h could reduce the standard deviation of contact force by 26.2% at maximum, and the optimization effect, optimal solution and optimization direction of some parameters were related to the running speed [Wu *et al.*, 2022]. The joint optimization of nine pantograph parameters based on non-dominated sorting GA-II at 120 km/h and 160 km/h, could reduce the standard deviation of contact force by 19.4% and 39.0%, respectively, and the optimization direction was to reduce m_3 and k_2 , increase c_2 , and the optimization direction of the remaining parameters was related to the running speed [Wang *et al.*, 2023].

Second, based on the pantograph–catenary dynamic calculation, the standard deviation of contact force of the preset sample set is calculated, and the data fitting is used to establish the relationship function between the standard deviation of contact force and the pantograph dynamic parameters. The optimal solution of parameter vector is obtained by solving the optimal value of the function. Quadratic functions of the standard deviation of contact force on several pantograph parameters were established by the response surface method or Pseudo-monte Carlo method [Lee *et al.*, 2012; Su *et al.*, 2022; Wang *et al.*, 2017].

The above studies show that the running speed, the type and parameters of catenary, the reference value of pantograph parameters, the number and combination of parameters to be optimized have significant effects on the optimization effect and the optimal solution and that the optimization direction of some pantograph parameters may be completely opposite. Therefore, for a pantograph–catenary system involving running speed and dozens of pantograph–catenary parameters, it is necessary to explore the law of the response of pantograph–catenary coupling performance to pantograph parameters and obtain a method for pantograph parameter optimization that is not specific to a certain operating condition but has universal applicability. This is one of the important directions in the development of multi-parameter optimization methods for pantograph–catenary dynamics.

GA [Holland, 1975] has gained more applications in the field of joint multi-parameter optimization of pantographs [Wu *et al.*, 2022; Ambrósio *et al.*, 2013; Gregori *et al.*, 2018]. GA is a classical swarm intelligence optimization algorithm, whose selection operator simulates the rule of “survival of the fittest” in nature, adaptively adjusting the search direction during the process of optimizing, giving priority to individuals with small objective function value and improving the convergence rate. Meanwhile, taking into account that the individuals with large objective function value also have the possibility to enter the next generation, GA avoids falling into local optimal solutions too early. However, GA requires more adjustable parameters, and is less convenient and less accurate than new swarm intelligence

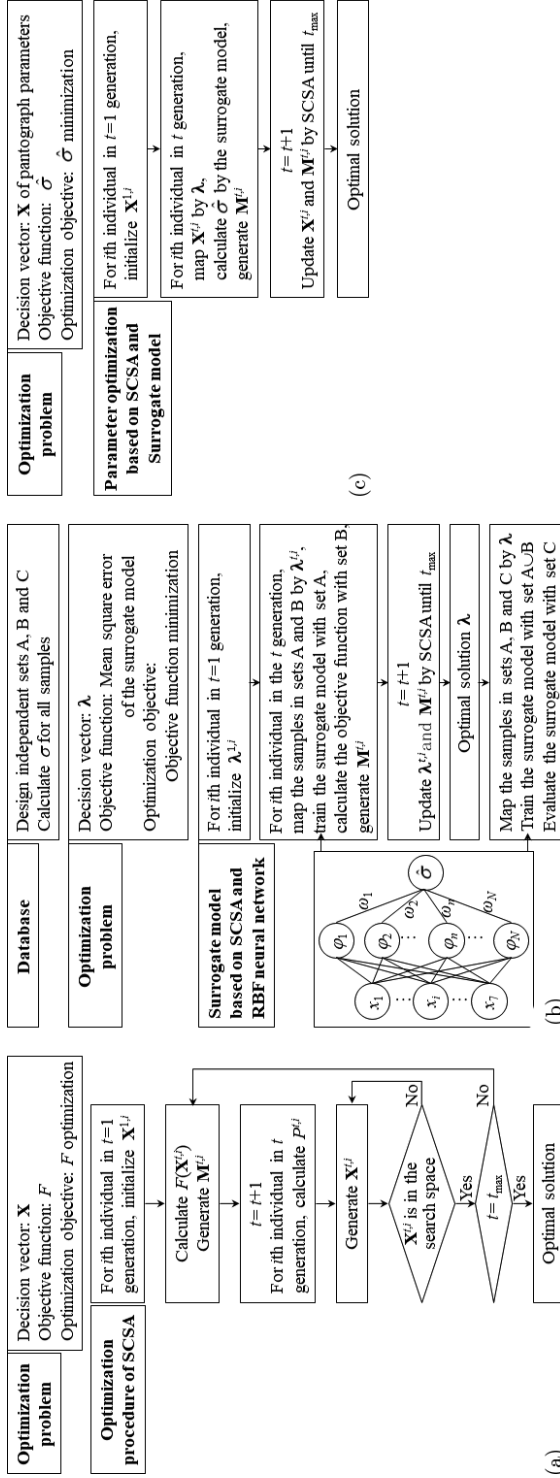


Fig. 1. Computational procedure, (a) SCSA, (b) Surrogate model based on SCSA and RBF neural network and (c) Parameter optimization based on SCSA and Surrogate model.

algorithms such as crow search algorithm (CSA) [Askarzadeh, 2016], which can be used to solve complex, high-dimensional and multimodal optimization problems due to the diversity of search areas, higher probability of escaping from local optimal solutions and more convenient application [Arora *et al.*, 2019]. In addition, CSA also suffers from slow convergence rate [Sayed *et al.*, 2019] and lack of local search efficiency [Arora *et al.*, 2019].

In this paper, selective crow search algorithm (SCSA) was proposed for solving the optimization problems of multiple pantograph dynamic parameters by introducing the selection operator from GA into CSA. Based on the pantograph–catenary dynamic model, a database of the standard deviation of contact force was constructed for the running speed and six pantograph parameters. Combining the radial basis function (RBF) neural network [Broomhead and Lowe, 1988] and SCSA, a surrogate model for the standard deviation of contact force with high generalization ability was developed. Based on the surrogate model and SCSA, 63 combinations of pantograph dynamics parameters were optimized at two filtering frequencies and five running speeds, and a generalized method for optimizing high-speed pantograph dynamics parameters was proposed (Fig. 1).

2. Selective Crow Search Algorithm

CSA is a meta-heuristic algorithm based on the foraging behavior rule of crows, whereby crows in a population memorize their food storage places, maintain a certain probability of preventing food from being stolen by other crows, and preferentially track other counterparts in the population in order to try to steal food from their storage places. The food storage places correspond to the memory coordinates of the algorithm. Unlike CSA, where all individuals have the same probability of being tracked, SCSA sets individuals to preferentially track their counterparts with lower objective function values at the memory coordinates.

The first step is to set the dimension and search space of decision vector, the maximum number of iterations t_{\max} , population size I , the flight length a and the awareness probability b . The second step is to initialize the position $\mathbf{X}^{1,i}$ and the memory $\mathbf{M}^{1,i}$ of the i th ($i = 1, 2, \dots, I$) individual in the first generation. $\mathbf{X}^{1,i}$ is randomly generated in the search space of decision vector, and $F(\mathbf{X}^{1,i})$ is obtained by substituting $\mathbf{X}^{1,i}$ into the objective function. At this point, the memory $\mathbf{M}^{1,i}$, i.e., the best position of the individual during the iteration, are the same as $\mathbf{X}^{1,i}$. In the third step, the position $\mathbf{X}^{t,i}$ of the i th individual in the t th ($t = 2, \dots, t_{\max}$) generation are generated. Referring to the roulette algorithm [Jebari and Madiafi, 2013], the probability of the i th individual being tracked is related to $F(\mathbf{M}^{t-1,i})$ of its memory.

$$P^{t,i} = 1 - F(\mathbf{M}^{t-1,i}) / \sum_{k=1}^I F(\mathbf{M}^{t-1,k}). \quad (2.1)$$

The tracking target of the i th individual is drawn as the j th individual by unequal probability sampling. If the random number generated within $[0, 1]$ is less than the

awareness probability, it means that the tracking of the i th individual is found by the j th individual, and its position is updated to the random position in the search space; conversely, if the tracking of the i th individual is not found by the j th individual, and the i th individual moves from its own position $\mathbf{X}^{t-1,i}$ to the direction of the memory $\mathbf{M}^{t-1,i}$ of the j th individual, and its positions are updated to

$$\mathbf{X}^{t,i} = \mathbf{X}^{t-1,i} + a\xi^i(\mathbf{M}^{t-1,j} - \mathbf{X}^{t-1,i}), \quad \xi^j \geq b \quad (2.2)$$

where the second term is the movement distance, which is related to the flight distance a and the random number ξ^i . The larger the a , the larger the distance moved and the wider the search range. ξ^i and ξ^j are random numbers uniformly distributed in the interval $[0, 1]$, and ξ^i makes the distance moved somewhat random. The awareness probability b characterizes the intensification and diversification of an individual's search region. When the value is small, individuals tend to search in the vicinity of the better position of the current area, reflecting intensification; conversely, they tend to search globally, reflecting diversification. In addition, the new position of individuals in CSA may be located outside the search space, and SCSA proposes to re-extract the tracked individuals and track the new position until they are within the search space. $F(\mathbf{X}^{t,i})$ of the i th individual is obtained by substituting

Table 1. Function value at the optimal solution obtained by different swarm intelligence optimization algorithm.

Expression of test functions [Rahnamayan <i>et al.</i> , 2007]	Value ranges of x_r	Function value at the optimal solution					
		SCSA		CSA		GA	
		Aver.	Std.	Aver.	Std.	Aver.	Std
Quartic function: $\sum_{r=1}^6 rx_r^4/10^{-36}$	$[-1.28, 1.28]$	3.79	7.42	59.3	96.0	7.83×10^{20}	9.91×10^4
Sumpower function: $\sum_{r=1}^6 x_r ^{r+1}/10^{-25}$	$[-10,10]$	1.42	1.86	7.36	11.0	3.73×10^{18}	4.69×10^{10}
Alpine function: $\sum_{r=1}^6 x_r \sin x_r + 0.1x_r /10^{-10}$	$[-10, 10]$	4.10	1.92	30.2	15.4	2.95×10^7	2.22×10^7
Levy function: $\{\sin^2(3\pi x_1) + (x_6 - 1)^2 [1 + \sin^2(2\pi x_6)] + \sum_{r=1}^5 (x_r - 1)^2 [1 + \sin^2(3\pi x_{r+1})]\}/10^{-17}$	$[-10, 10]$	4.11	3.68	39.1	39.8	1.73×10^{12}	1.36×10^{-3}

Table 2. Parameters of the optimization algorithm.

Algorithm	Parameter	Value
GA	Population size	50
	Chromosomes number	140
	Crossover probability	0.99
	Mutation probability	0.005
CSA	Population size	50
SCSA	Flight length	2
	Awareness probability	0.1

$\mathbf{X}^{t,i}$ into the objective function. If the objective function value of its new position is lower than $\mathbf{M}^{t-1,i}$, then $\mathbf{M}^{t,i} = \mathbf{X}^{t,i}$; otherwise, $\mathbf{M}^{t,i} = \mathbf{X}^{t-1,i}$. Finally, iterate to the t_{\max} -th generation and repeat to update the position of all individuals, calculate the objective function value and update the memory. The memory with the smallest objective function value among all individuals are extracted, i.e., the optimal solution of the decision vector.

GA, CSA and SCSA were used to solve for the global optimal solution of four 6-dimensional test functions (Table 1), Quartic, Sumpower, Alpine and Levy, all of which have a theoretical solution of 0 at the global optimal solution. 2000 generations were taken as the maximum number of iterations, and the other computation parameters are shown in Table 2. Within the search space, Quartic and Sumpower are unimodal functions, while Alpine and Levy are multimodal functions with multiple local minimum value. To avoid accidental errors due to random terms in the algorithms, each algorithm run 100 times independently on each test function and the mean, and standard deviation of the function values at the optimal solution was calculated. For the same test function, the function value at the optimal solution obtained by the SCSA optimization and its dispersion are both one order of magnitude smaller than the CSA case and closer to the theoretical value of 0. In addition, the solving accuracies of CSA and SCSA are higher than that of the GA.

3. Optimization of Surrogate Model by RBF Neural Network

The flowchart of obtaining the surrogate model of the standard deviation of contact force using SCSA-RBF network is shown in Fig. 1(b). First, a sample set containing 4000 cases of pantograph–catenary interaction was constructed based on Latin hypercube sampling and verified pantograph–catenary finite element model. Then, using the RBF neural network trained by SCSA, the surrogate model was established, and its generalization ability was evaluated.

3.1. Construction of surrogate model

The decision vector was selected to consist of the running speed v and six pantograph three-mass parameters, i.e., $\mathbf{X} = \{v, m_3, m_2, m_1, k_3, k_2, c_1\}^T$. The value range for decision variable X_r ($r = 1, 2, \dots, 7$) was determined according to the engineering practice (Column 3 of Table 3). Set $k_1 = 74 \text{ N/m}$, $c_3 = 50 \text{ N} \cdot \text{s/m}$ and $c_2 = 10 \text{ N} \cdot \text{s/m}$. Further, \mathbf{x} was obtained by processing \mathbf{X} through some mapping.

The RBF neural network was used to construct a surrogate model of the standard deviation of contact force at a low-pass filtering frequency of 20 Hz or 40 Hz with respect to \mathbf{x} . Each x_r of \mathbf{x} corresponds to a neuron of the input layer, and the predictive value $\hat{\sigma}(\mathbf{x})$ of surrogate model for the standard deviation of contact force can be expressed as follows:

$$\hat{\sigma}(\mathbf{x}) = \sum_{n=1}^N \varphi_n \omega_n, \quad (3.1)$$

Table 3. Value range and reference value of variables.

Variable	Unit	Value range	Reference value
v	km/h	[250, 450]	/
m_3	kg	[5, 11]	7.94
m_2	kg	[5, 20]	8.22
m_1	kg	[3, 20]	5.90
k_3	N/m	[4000, 14000]	6650
k_2	N/m	[8000, 20000]	13181
c_1	N · s/m	[10, 240]	67.41

where $\varphi_n = \varphi(\|\mathbf{x} - \mathbf{x}_n\|)$ is the RBF value between \mathbf{x} and \mathbf{x}_n , which corresponds to a neuron of the hidden layer; $\|\mathbf{x} - \mathbf{x}_n\|$ is the Euclidean distance between \mathbf{x} and the n th sample \mathbf{x}_n in the training set; ω_n is the weight coefficient of \mathbf{x}_n and the vector of weight coefficients satisfies

$$\begin{bmatrix} \omega_1 \\ \vdots \\ \omega_n \\ \vdots \\ \omega_N \end{bmatrix} = \begin{bmatrix} \varphi_{11} & \cdots & \varphi_{1m} & \cdots & \varphi_{1N} \\ \vdots & & \vdots & & \vdots \\ \varphi_{n1} & \cdots & \varphi_{nm} & \cdots & \varphi_{nN} \\ \vdots & & \vdots & & \vdots \\ \varphi_{N1} & \cdots & \varphi_{Nm} & \cdots & \varphi_{NN} \end{bmatrix}^{-1} \begin{bmatrix} \sigma_1 \\ \vdots \\ \sigma_n \\ \vdots \\ \sigma_N \end{bmatrix}, \quad (3.2)$$

where $\varphi_{nm} = \varphi(\|\mathbf{x}_n - \mathbf{x}_m\|)$ is the RBF value between two samples \mathbf{x}_n and \mathbf{x}_m in the training set, and σ_n is the theoretical value of the standard deviation of contact force corresponding to \mathbf{x}_n . Among them, $n = 1, \dots, N$ and $m = 1, \dots, N$, where N is the number of samples in the training set, and the RBF $\varphi(x) = x^2 \ln x$ [Bookstein, 1989]. Based on the standard deviation of contact force of all samples in the training set, the weight coefficient of each sample is calculated according to Eq. (3.2) and substituted into Eq. (3.1) to obtain the predictive value of surrogate model for the standard deviation of contact force with respect to any unknown sample.

3.2. Training and assessing of surrogate model

The Latin hypercube sampling method [Mckay and Conover, 1979] was used to draw 4000 samples in a seven-dimensional sample space of \mathbf{X} . The sample set was divided into three disjoint sets A, B and C with sample sizes of 2200, 900 and 900, respectively. The statistical results showed that all decision variables in the three sets were approximately uniformly distributed.

Based on the catenary finite element and pantograph three-mass model [Wu *et al.*, 2021, 2022], dynamic calculations were carried out to obtain the time domain curves of contact force for the above 4000 samples. The time domain curves of contact force were low-pass filtered at 20 Hz and 40 Hz to obtain the theoretical values of the standard deviation of contact force, and then a database of the standard deviation of contact force at the two low-pass filtering frequencies was

obtained. In dynamic calculation, the deviation ΔF_m between the average contact force F_m and the upper limit of empirical value $70 + 0.00097v^2$ [European Parliament, 2012b] was less than 0.5 N by adjusting the lifting force exerted on the mass block. The kernel density estimation method [Emanuel, 1962] was used to calculate the probability density curve of ΔF_m for the 4000 samples, and the interval of ΔF_m within the probability of 0.95 was about $[-0.38, 0.31]$ N.

Map the decision variable X_r of all samples of a given set to the interval $[0, \lambda_r]$, i.e.,

$$x_r = \frac{X_r - X_{r \min}}{X_{r \max} - X_{r \min}} \cdot \lambda_r, \tag{3.3}$$

where $X_{r \min}$ and $X_{r \max}$ are, respectively, the lower limit and upper limit of X_r in the value space (Column 3 of Table 3). The common mapping method is the normalization [Qin *et al.*, 2014], which takes the upper limit of the mapping interval $\lambda_r = 1$. The surrogate model was trained by using the unions of sets A and B as the training sets.

This paper proposes to obtain the upper limit of mapping interval λ_r based on SCSA. With the minimum mean square error [Alpaydin, 2014] of the surrogate model on the validation set as the optimization objective, the optimal solution of $\lambda = \{\lambda_1, \lambda_2, \dots, \lambda_7\}^T$ was solved through SCSA. The specific steps are as follows:

- (1) Set the value range of λ_r as $[0, 10]$ and the maximum number of iterations as 200, and the other computation parameters are shown in Table 2.
- (2) The position $\lambda^{1,i}$ of the i th ($i = 1, 2, \dots, N$) individual in generation 1, which are also its memory, is generated in the 7-dimensional value space by using the Latin hypercube method. The mapping process of Eq. (3.3) is performed on the training set A and the validation set B. N surrogate models of the standard deviation of contact force in generation 1 are obtained based on the training set, and the validation errors of these surrogate models are obtained based on the validation set.
- (3) The position $\lambda^{t,i}$ of the i th individual in generation t ($t = 2, \dots, 200$) is generated according to the updated position criterion in SCSA, and the mapping process is repeated for sets A and B, training the surrogate model, calculating the validation error and generating the memory. The optimal solution, i.e., the value λ corresponding to the minimum value of the validation error, is extracted (Table 4).

Table 4. λ_r obtained by SCSA.

Cut-off frequency (Hz)	λ_1	λ_2	λ_3	λ_4	λ_5	λ_6	λ_7
20	9.839	0.375	0.431	0.378	0.528	0.254	0.417
40	9.473	0.320	0.406	0.365	0.483	0.247	0.408

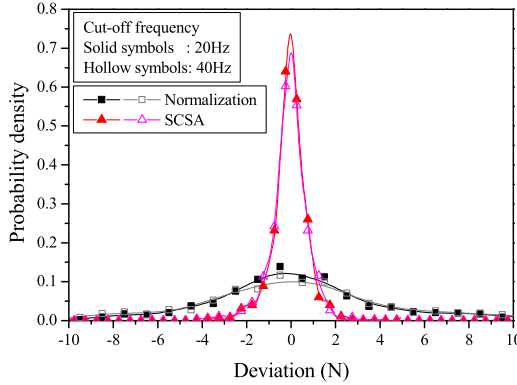


Fig. 2. Probability density distribution of the error of the surrogate models on the test set.

Table 5. Prediction error of the surrogate model on the test set.

Mapping method	Cut-off frequency (Hz)	Distribution interval (N)	Mean squared error (N^2)	Coefficient of determination
Normalization	20	$[-16.3, 12.1]$	36.697	0.764
	40	$[-16.3, 13.2]$	41.054	0.864
SCSA optimization	20	$[-2.1, 1.5]$	0.676	0.996
	40	$[-2.1, 1.5]$	0.728	0.998

- (4) The final surrogate model is obtained by mapping the training and test sets with the optimal solution of λ , using the unions of sets A and B as the training set.

The prediction error of the surrogate model is usually calculated based on the test set samples, and the distribution interval of error, mean squared error and coefficient of determination are usually used to characterize the generalization ability of surrogate model [Qin *et al.*, 2014]. For the sample \mathbf{x}_p in test set, the surrogate model-predicted value $\hat{\sigma}_p$ of the standard deviation of contact force and the error $\hat{\sigma}_p - \sigma_p$ was calculated. The interval of the surrogate model error within the probability of 0.95, the mean square error $\sum_{p=1}^{900} (\hat{\sigma}_p - \sigma_p)^2 / 900$ [Alpaydin, 2014], and the coefficient of determination $1 - \sum_{p=1}^{900} (\hat{\sigma}_p - \sigma_p)^2 / \sum_{p=1}^{900} (\sigma_p - \bar{\sigma})^2$ [Nagelkerke, 1991] were calculated, where σ_p is the FEM calculated value of the standard deviation of contact force, and $\bar{\sigma}$ is their average value.

3.3. Generalization and calculation efficient of surrogate model

Whether under the low-pass filtering frequency of 20 Hz or 40 Hz, the upper limits of decision variables mapping interval were set as 1 or determined by SCSA, and the resulting surrogate models on the test set C all had errors that obey a normal distribution (Fig. 2). The interval of the errors within the probability of 0.95 was about $[-16.3, 12.7]$ N and $[-2.1, 1.5]$ N, the mean squared errors were about

38.9 N² and 0.7 N², and the coefficients of determination were about 0.814 and 0.997, respectively (Table 5). Obviously, the generalization ability of the surrogate model obtained after mapping the decision vector by using the normalization method is weak. Comfortingly, the SCSA optimization method in this paper to determine the upper limit of the mapping interval can significantly reduce the prediction error of the surrogate model for new samples and improve the generalization ability of the surrogate model.

In addition, when calculating the standard deviation of contact force for a single sample, the surrogate model required 3.1×10^{-7} core hours, which is only $1/10^8$ of the time for calculation with the pantograph–catenary dynamic simulation, i.e., 10 core hours. Therefore, the computational efficiency is improved greatly.

4. Optimization of Pantograph Parameters by Surrogate Model

4.1. Optimization problem and decision vector

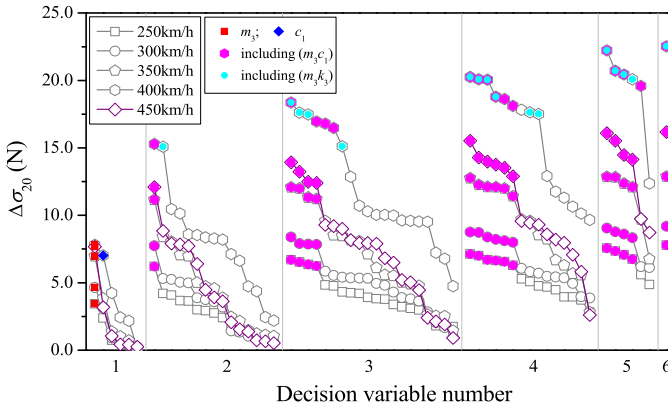
With the objective of minimizing the standard deviation of contact force at a given low-pass filtering frequency and running speed, the optimal solution of decision vector was obtained by using SCSA. Among them, set low-pass filtering frequencies as 20 Hz and 40 Hz, and speeds as 250, 300, 350, 400, 450 km/h. The decision vector is a combination of 6 pantograph parameters regarding m_3, m_2, m_1, k_3, k_2 and c_1 when the number of decision variables is $r = 1, 2, 3, 4, 5$ and 6, the number of decision vectors is $C_6^1 = 6, C_6^2 = 15, C_6^3 = 20, C_6^4 = 15, C_6^5 = 6$ and $C_6^6 = 1$, respectively, totaling $\sum_{r=1}^6 C_6^r = 63$. It means that optimization iterations should be conducted for a total of 630 combinations. The standard deviation of contact force of different decision vector is calculated by surrogate model. The value ranges of decision variables are shown in Table 3, the maximum number of iterations is 200, and the relevant parameters of optimization algorithm are shown in Table 2. The optimization problem can be described as follows:

$$\begin{aligned} & \min \hat{\sigma}(\mathbf{X}) \\ & \mathbf{X} = \{m_3, m_2, m_1, k_3, k_2, c_1\}^T \\ & \text{s.t.} \begin{cases} 5 \text{ kg} \leq m_3 \leq 11 \text{ kg} \\ 5 \text{ kg} \leq m_2 \leq 20 \text{ kg} \\ 3 \text{ kg} \leq m_1 \leq 20 \text{ kg} \\ 4000 \text{ N/m} \leq k_3 \leq 14000 \text{ N/m} \\ 8000 \text{ N/m} \leq k_2 \leq 20000 \text{ N/m} \\ 10 \text{ N} \cdot \text{s/m} \leq c_1 \leq 240 \text{ N} \cdot \text{s/m} \end{cases} \end{aligned} \tag{4.1}$$

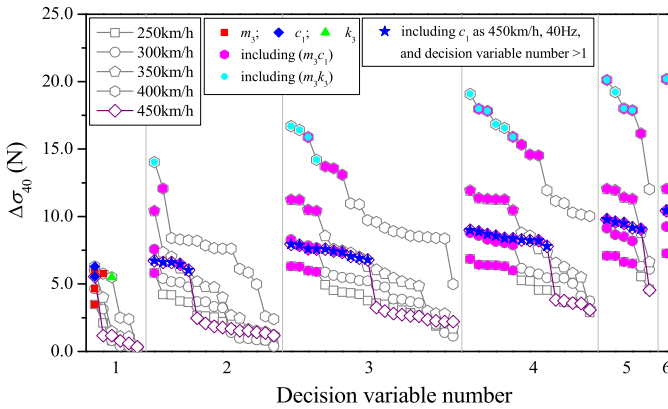
Table 6 shows the ratio of convergent data, final convergence values and the number of iterations, t_0 , required to solve the above 630 combinations, of GA and SCA to SCSA. The final convergence value is the objective function value of the t_{\max} generation, the relative deviation between the objective function value of generation

Table 6. Ratio of convergent data of GA and CSA to SCSA.

Number of decision variables	Ratio of the final convergence values		Ratio of the number of iterations	
	GA/SCSA	CSA/SCSA	GA/SCSA	CSA/SCSA
6	1.005 ± 0.008	1.004 ± 0.009	2.9 ± 2.4	1.7 ± 0.8
5	1.000 ± 0.002	1.001 ± 0.010	1.9 ± 1.0	1.4 ± 0.4
4	1.000 ± 0.002	1.000 ± 0.002	2.3 ± 4.2	1.7 ± 1.7
3	1.000 ± 0.001	1.000 ± 0.000	2.4 ± 3.0	1.7 ± 1.9
2	1.000 ± 0.001	1.000 ± 0.000	2.1 ± 3.3	1.6 ± 1.7
1	1.000 ± 0.000	1.000 ± 1.000	1.0 ± 0.0	1.0 ± 0.0



(a)



(b)

Fig. 3. (a) $\Delta\sigma_{20}$ and (b) $\Delta\sigma_{40}$ of the optimal solution of all decision vectors.

$t \geq t_0$ and the final convergence value is not more than 1%. For the same operating conditions, the convergence values obtained with SCSA are slightly lower than those of GA and CSA, and the number of iterations is about 1/2 of those of the latter two algorithms.

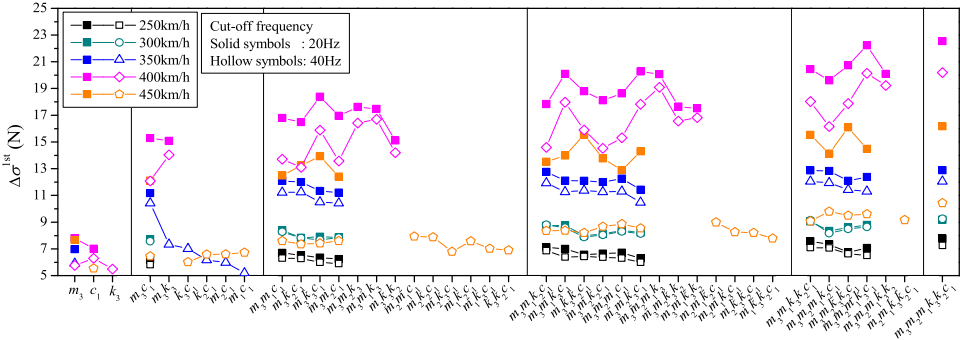


Fig. 4. First vectors and $\Delta\sigma^{1st}$.

Table 7. Common parameters among first vectors and their optimization directions.

Velocity		250 km/h	300 km/h	350 km/h	400 km/h	450 km/h
Cut-off frequency	20 Hz	$m_3 \downarrow$	$m_3 \downarrow$	$m_3 \downarrow (m_3 \downarrow, c_1 \uparrow)$	$m_3 \downarrow, c_1 \uparrow$	$m_3 \downarrow$
	40 Hz	$m_3 \downarrow$	$m_3 \downarrow$	$m_3 \downarrow, c_1 \uparrow$	$m_3 \downarrow, k_3 \uparrow$	$(m_3 \downarrow, c_1 \uparrow)$
		$(m_3 \downarrow, c_1 \uparrow)$	$(m_3 \downarrow, c_1 \uparrow)$	$(m_3 \downarrow, c_1 \uparrow)$	$m_3 \downarrow, c_1 \uparrow, k_3 \uparrow$	$c_1 \uparrow$
			$(m_3 \downarrow, c_1 \uparrow)$	$(m_3 \downarrow, c_1 \uparrow)$	$(m_3 \downarrow, c_1 \uparrow)$	$(c_1 \uparrow)$
					$(m_3 \downarrow, k_3 \uparrow)$	

4.2. Influence of variable combinations on optimization effect

Using the existing DSA380 pantograph in service as the reference (Column 4 of Table 3), the drop-out value $\Delta\sigma$ of the standard deviation of contact force corresponding to the optimal solution of 63 decision vectors was calculated at two filtering frequencies and five speeds. $\Delta\sigma_{20}$ (Fig. 3(a)) and $\Delta\sigma_{40}$ (Fig. 3(b)) of different combinations of decision variables with the same filtering frequency, speed and number of decision variables were arranged in descending order. For the same filtering frequency, speed and number of decision variables, $\Delta\sigma$ decreased in a stepwise manner with respect to the combining form of decision variables, and the decision vector of the first step is taken as a first vector (solid symbols in Fig. 3). The larger the $\Delta\sigma$ is, the more significant the optimization effect is. Therefore, the first vector represents the optimal combination of parameters for the same filtering frequency, speed and number of decision variables, and the drop-out value $\Delta\sigma^{1st}$ of the standard deviation of contact force represents the best optimization effect.

Figure 4 shows first vectors and their $\Delta\sigma^{1st}$ of all working conditions, and Table 7 shows common parameters and their optimization direction of first vectors. If the number of decision variables is 1, at a speed of 350 km/h or below, m_3 is rated as level 1 at both filtering frequencies; at 400 km/h, m_3 and c_1 are rated as level 1 at both filtering frequencies and k_3 is rated as level 1 at 40 Hz; at 450 km/h, m_3 is rated as level 1 at 20 Hz and c_1 is rated as level 1 at 40 Hz. If the number of decision variables is between 2 and 5, at a speed of 400 km/h or below, all decision vectors containing (m_3, c_1) are rated as level 1 at both filtering frequencies, and all decision

vectors containing (m_3, k_3) are also rated as level 1 at 400 km/h; at 450 km/h, all decision vectors containing (m_3, c_1) are rated as level 1 at 20 Hz, and all decision vectors containing c_1 are rated as level 1 at 40 Hz. Among these first vectors, the optimization direction of m_3, m_1 and c_1 does not change with cut-off frequency and speed, and has the common feature of decreasing m_3 and m_1 and increasing c_1 . The optimization direction of k_3 only decreases at 450 km/h and 40 Hz and increases in all other working conditions, while the optimization direction of k_2 and m_2 is related to the filter cut-off frequency and speed.

The ratio of $\Delta\sigma^{1st}$ of the first vectors for the number of decision variables between 1 and 5 to that for the number of decision variables of 6 was calculated (Fig. 5). The ratio was only 0.46 ± 0.08 for the number of decision variables of 1, and increased to $0.77 \pm 0.09, 0.82 \pm 0.07, 0.88 \pm 0.55$ and 0.93 ± 0.02 , respectively, when the number of decision variables increased from 2 to 5. In other words, the larger the number of decision variables, the larger the $\Delta\sigma^{1st}$, i.e., the better the optimization effect at different speeds and filtering frequencies. The effect of optimization of a single pantograph dynamics parameter is much lower than that of multi-parameter joint optimization, and the effect of five-parameter optimization is comparable to that of six-parameter optimization.

Therefore, it is recommended that several pantograph parameters be jointly optimized, with priority given to reducing m_3 and increasing c_1 , and also to increasing k_3 at 400 km/h. The optimization directions of m_1, k_3, m_2 and k_2 are significantly influenced by the filtering frequency and train running speed and need to be determined according to the actual engineering conditions.

One phenomenon to be noted here is that at 350 km/h or below, $\Delta\sigma_{40}^{1st}$ and $\Delta\sigma_{20}^{1st}$ are close to each other, and the maximum difference between the two is only 1.1 N. The effect of low-pass filtering frequency on the optimization of the standard deviation of contact force is negligible. At 400 km/h and above, the $\Delta\sigma_{40}^{1st}$ is lower than its $\Delta\sigma_{20}^{1st}$, and the maximum difference between the two is up to 7.3 N, and

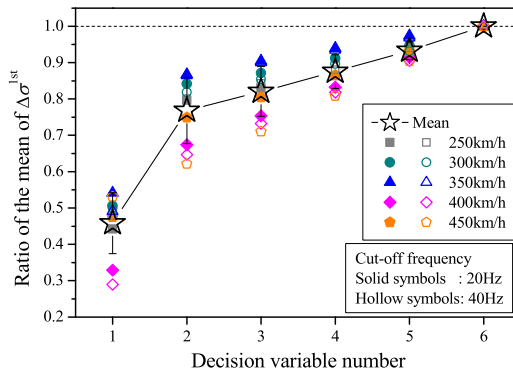


Fig. 5. Ratio of the mean of $\Delta\sigma^{1st}$ versus the number of decision variables.

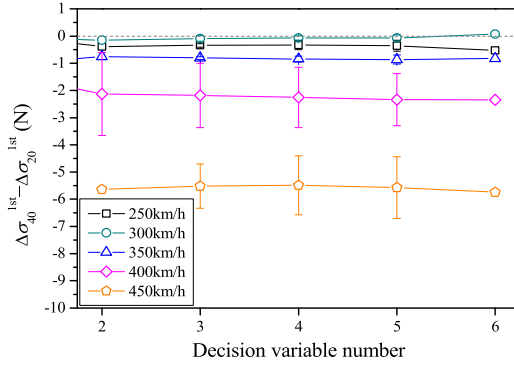


Fig. 6. $\Delta\sigma_{40}^{1st} - \Delta\sigma_{20}^{1st}$ for different velocities and number of decision variables.

the larger the speed, the greater the effect of filtering frequency on the optimization effect of the standard deviation of contact force (Fig. 6).

4.3. Spectral analysis of optimized contact force

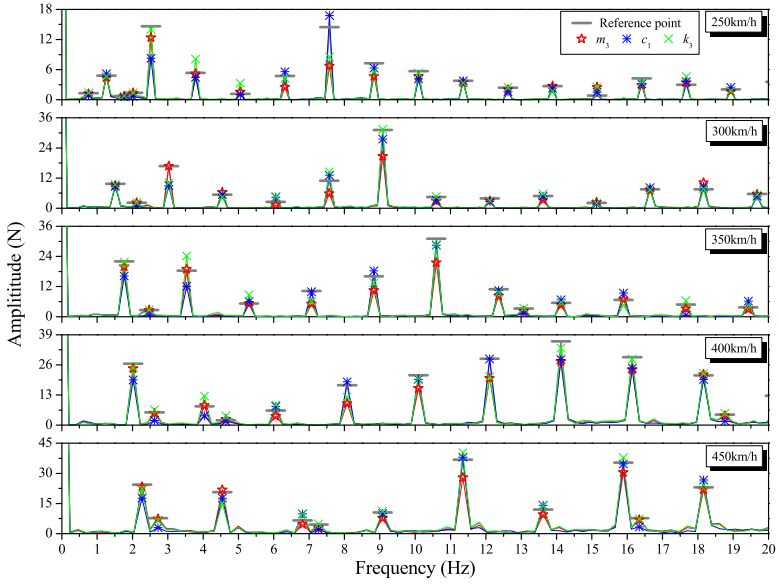
Figure 7 represents the contact force spectral of the reference value, and the optimal solutions of m_3 , k_3 and c_1 . The standard deviation of the contact force within frequency interval $f_1 - f_2$ can be described by the contact force amplitude $G(f)$ at the peak frequency f [Oppenheim *et al.*, 2006],

$$\sigma_{f_1-f_2} = \sqrt{\sum_{f=f_1}^{f_2} G(f)^2/2}. \quad (4.2)$$

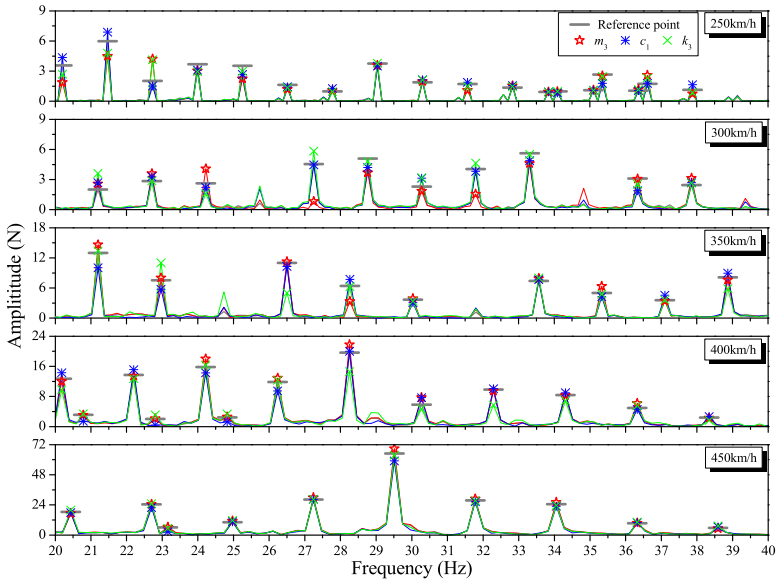
Set $\Delta\sigma_{f_1-f_2}$ as the descent value from the reference value of $\sigma_{f_1-f_2}$.

For the frequency interval of 0–20 Hz (Fig. 7(a)), the optimal solutions for m_3 and for combinations containing (m_3, c_1) at five speeds, and the optimal solutions for c_1 and for combinations containing (m_3, k_3) at 400 km/h, their $\Delta\sigma_{0-20}$ are several times larger than those in the case of the optimal solutions for other decision vectors at the same speed. In addition, the $\Delta\sigma_{5-20}$ is several times $\Delta\sigma_{0-5}$ for the optimal solution for m_3 at five speeds, which means optimizing m_3 mainly leads to a decrease in the frequency amplitude at the peak of frequency spectrum in the range of 5–20 Hz. The $\Delta\sigma_{0-5}$ and $\Delta\sigma_{5-20}$ of the optimal solutions for c_1 at 400 km/h are comparable, but $\Delta\sigma_{0-5}$ is several times larger than $\Delta\sigma_{5-20}$ at other four velocities, which means optimizing c_1 mainly leads to a decrease in the frequency amplitude at the peak of frequency spectrum in the range of 0–5 Hz. The $\Delta\sigma_{0-5}$ and $\Delta\sigma_{5-20}$ of the optimal solutions for combinations containing (m_3, c_1) at five velocities are comparable. Optimizing the combinations containing (m_3, k_3) mainly leads to a decrease in the frequency amplitude at the peak of frequency spectrum in the range of 5–20 Hz.

For the frequency interval of 20–40 Hz (Fig. 7(b)), $\Delta\sigma_{0-40}$ of the optimal solution of k_3 at 400 km/h is comparable to that in the case of the optimal solutions of m_3



(a)



(b)

Fig. 7. Spectrum of pantograph–catenary contact force.

and m_1 at the same speed. Therefore, for a low-pass filtering frequency of 40 Hz and a speed of 400 km/h, k_3 and all vectors containing (m_3, k_3) become first vectors. $\Delta\sigma_{20-40}$ of the optimal solution of c_1 at 450 km/h is several times larger than that in the case of the optimal solutions of other parameters at the same running speed, while the optimal solution of m_3 is a large and positive value. Therefore, for a low-pass filtering frequency of 40 Hz and 450 km/h, c_1 and all vectors contained (c_1) become first vectors. At other working conditions for a low-pass filtering frequency of 40 Hz, $\Delta\sigma_{20-40}$ are close to 0, therefore the level 1 vectors are the same as at 20 Hz.

5. Conclusion

The following are the main conclusions of this paper:


- (1) A novel optimization algorithm called SCSA is proposed by employing the selection operator from GA during the process of CSA. It has been validated that the solution accuracy and convergence rate of SCSA are better than GA and CSA.
- (2) A database is constructed by Latin hypercube sampling method and verified pantograph–catenary finite element model, and a surrogate model of the standard deviation of contact force with respect to the running speed and pantograph dynamic parameters is constructed by SCSA-RBF network. The decision variables need to be mapped. Different from normalization, the upper limits of mapping interval of the decision variables are gained by SCSA. It has been validated that the generalization ability of this method is much better than the normalization method.
- (3) Combining SCSA and surrogate model, with the optimization objective of minimizing the standard deviation of contact force, a total of 630 combinations of pantograph dynamic parameters are optimized considering the running speed of 250–450 km/h, the low-pass filtering frequency of 20 Hz and 40 Hz, and the traversal of all decision vectors. Then, a generalized method for optimizing high-speed pantograph dynamics parameters is proposed.


Overall, priority should reduce m_3 while increasing c_1 which can optimize current collection quality efficiently and significantly when optimizing pantograph dynamic parameters. The optimization effect and optimization direction of other parameters are relevant to running speed, cut-off frequency, reference value, etc., and need to be determined according to the specific working condition.

Acknowledgment

The authors gratefully acknowledge the support provided by the National Natural Science Foundation of China (No. 11672297).

ORCID

Rui Zhou  <https://orcid.org/0009-0000-8067-7027>

Xianghong Xu  <https://orcid.org/0000-0003-0739-5423>

References

- Alpaydin, E. [2014] *Introduction to Machine Learning*, 3rd edn. (The MIT Press, England).
- Ambrósio, J., Pombo, J. and Pereira, M. [2013] “Optimization of high-speed railway pantographs for improving pantograph-catenary contact,” *Theoretical & Applied Mechanics Letters* **3**(1), 013006.
- Arora, S., Singh, H., Sharma, M., Sharma, S. and Anand, P. [2019] “A new hybrid algorithm based on Grey Wolf optimization and Crow search algorithm for unconstrained function optimization and feature selection,” *IEEE Access* **7**(NOV), 26343–26361.
- Askarzadeh, A. [2016] “A novel metaheuristic method for solving constrained engineering optimization problems: Crow search algorithm,” *Computers & Structures* **169**(NOV), 1–12.
- Bookstein, F. L. [1989] “Thin-plate splines and the decomposition of deformations,” *IEEE Transactions on Pattern Analysis and Machine Intelligence* **16**(6), 567–585.
- Broomhead, D. S. and Lowe, D. [1988] “Radial basis functions, multi-variable functional interpolation and adaptive networks,” Memorandum Report No. ADA196234, Royal Signals and Radar Establishment Malvern (United Kingdom).
- Bruni, S. *et al.* [2018] “Pantograph-catenary interaction: recent achievements and future research challenges,” *International Journal of Rail Transportation* **6**(2), 57–82.
- Emanuel, P. [1962] “On estimation of a probability density function and mode,” *Annals of Mathematical Statistics* **33**(3), 1065–1076.
- European Parliament [2012a] “EN50317:2012: Railway applications-current collection systems-requirements for and validation of measurements of the dynamic interaction between pantograph and overhead contact line,” European Standard.
- European Parliament [2018] “EN50318:2018: Railway applications-current collection systems-validation of simulation of the dynamic interaction between pantograph and overhead contact line,” European Standard.
- European Parliament [2012b] “EN50367:2012: Railway applications-current collection systems-technical criteria for the interaction between pantograph and overhead line (to achieve free access),” European Standard.
- European Parliament [2020] “EN50367:2020: Railway applications-criteria to achieve technical compatibility between pantographs and overhead contact line,” European Standard.
- Gregori, S., Tur, M., Nadal, E. and Fuenmayor, F. J. [2018] “An approach to geometric optimisation of railway catenaries,” *Vehicle System Dynamics* **56**(8), 1162–1186.
- Holland, J. [1975] *Adaptation in Natural and Artificial Systems* (University of Michigan Press, Ann. Arbor).
- Jebari, K. and Madiafi, M. [2013] “Selection methods for genetic algorithms,” *International Journal of Emerging Science* **3**(4), 333–344.
- Kim, J. W., and Yu, S. N. [2013] “Design variable optimization for pantograph system of high-speed train;using robust design technique,” *International Journal of Precision Engineering and Manufacturing* **14**(2), 267–273.
- Lee, J. H., Kim, Y. G., Paik, J. S. and Park, T. W. [2012] “Performance evaluation and design optimization using differential evolutionary algorithm of the pantograph for

- the high-speed train,” *Journal of Mechanical Science and Technology* **26**(10), 3253–3260.
- Mckay, M. D. and Conover, R. J. B. J. [1979] “A comparison of three methods for selecting values of input variables in the analysis of output from a computer code,” *Technometrics* **21**(2), 239–245.
- Nagelkerke, N. J. D. [1991] “A note on a general definition of the coefficient of determination,” *Biometrika* **78**(3), 691–692.
- Oppenheim, A. V., Willsky, A. S. and Hamid S. [2006] *Signals and Systems*, 2nd edn. (Prentice-Hall, USA).
- Pombo, J. and Ambrósio, J. [2012] “Influence of pantograph suspension characteristics on the contact quality with the catenary for high speed trains,” *Computers & Structures* **110**(NOV), 32–42.
- Qin, Y., Zhang, Y., Cheng, X. Q., Jia, L. M. and Xing, Z. Y. [2014] “An analysis method for correlation between catenary irregularities and pantograph-catenary contact force,” *Journal of Central South University* **21**(8), 3353–3360.
- Rahnamayan, S., Tizhoosh, H. R. and Salama, M. M. A. [2007] “A novel population initialization method for accelerating evolutionary algorithms,” *Computers & Mathematics with Applications* **53**(10), 1605–1614.
- Sayed, G. I., Hassaniien, A. E. and Azar, A. T. [2019] “Feature selection via a novel chaotic crow search algorithm,” *Neural Computing & Applications* **31**(1), 171–188.
- Su, K. X., Zhang, J. W., Zhang, J. W., Yan, T. and Mei, G. M. [2022] “Optimisation of current collection quality of high-speed pantograph-catenary system using the combination of artificial neural network and genetic algorithm,” *Vehicle System Dynamics* **61**(1), 260–285.
- Wang, X. Y., Nian, X. H., Chu, X. Y. and Yue, P. C. [2017] “Research on dynamic performance and parameter optimization of the high-speed pantograph and catenary system,” *2017 Prognostics and System Health Management Conference (Phm-Harbin)*, Harbin, China, pp. 486–491, <https://doi.org/10.1080/00423114.2022.2151921>.
- Wang, H. L., Zheng, D. Y., Huang, P. and Yan, W. Y. [2023] “Design optimisation of railway pantograph-catenary systems with multiple objectives,” *Vehicle System Dynamics*.
- Wu, M. Z., Liu, Y. and Xu, X. H. [2021] “Sensitivity analysis and optimization on parameters of high speed pantograph-catenary system,” *Chinese Journal of Theoretical and Applied Mechanics* **53**(1), 75–83.
- Wu, M. Z., Xu, X. H., Yan, Y. Z., Luo, Y., Huang, S. J. and Wang, J. S. [2022] “Multi-parameter joint optimization for double-strip high-speed pantographs to improve pantograph-catenary interaction quality,” *Acta Mechanica Sinica* **38**(1), 521344.
- Zhou, N. and Zhang, W. H. [2010] “Investigation on dynamic performance and parameter optimization design of pantograph and catenary system,” *Finite Elements in Analysis and Design* **47**(3), 288–295.